

PACS 64.70.K-, 77.84.Bw, 81.30.-t

Nanograin boundaries and silicon carbide photoluminescence

S.I. Vlaskina¹, G.N. Mishinova³, V.I. Vlaskin⁴, V.E. Rodionov⁵, G.S. Svechnikov²

¹*Yeoju Institute of Technology (Yeoju University),*

338, Sejong-ro, Yeosu-eup, Yeosu-gun, Gyeonggi-do, 469-705 Korea, e-mail: businkaa@mail.ru

²*National Technical University of Ukraine "Igor Sikorsky Kyiv Polytechnic Institute"*

Av.Pobedi 37, Kyiv, Ukraine,

³*Taras Shevchenko Kyiv National University, 64, Volodymyrs'ka str., 01033 Kyiv, Ukraine*

⁴*Sensartech, 2540 Lobelia Dr., Oxnard, 93036 California, USA*

⁵*State Institution "Institute of Environmental Geochemistry, NAS of Ukraine"*

av. Academician Palladin, Kyiv 34a

Abstract. The luminescence spectra of SiC crystals and films with grain boundaries (GB) on the atomic level were observed. The GB spectra are associated with luminescence centers localized in areas of specific structural abnormalities in the crystal, without no reference to the one-dimensional layer-disordering. The zero-phonon part of GB spectra is always within the same energy range (2.890...2.945 eV) and does not fit in the dependence of its position in the energy scale on the percent of hexagonality as in the case of stacking faults (SF_i) and deep level (DL_i) spectra. The zero-phonon part 2.945...2.890 eV with a fine structure is better observed in crystals with the centers of origin growth of crystal, if $N_D - N_A \sim (2...8) \cdot 10^{16} \text{ cm}^{-3}$, $N_D \sim (2...7) \cdot 10^{17} \text{ cm}^{-3}$. The edge phonons of the Brillouin zone TA-46 meV, LA-77 meV, TO-95 meV and LO-104 meV are involved in development of the GB spectrum. This spectrum may occur simultaneously with the DL_i and SF_i ones. The GB spectra also occur after high temperature processing the β -phase (in the 3C-SiC) with appearance of the α -phase. The temperature range of observation is 4.2...40 K. There is synchronous thermal quenching of all elements in the fine structure. The thermal activation energy of quenching is $E_a^T \sim 7 \text{ meV}$.

Keywords: silicon carbide, nanocrystalline film, luminescence, grain boundaries.

Manuscript received 03.05.17; revised version received 01.08.17; accepted for publication 06.09.17; published online 09.10.17.

1. Introduction

Silicon carbide is a wide bandgap indirect semiconductor with variety of polytypes. Experimental results and theoretical calculations showed that the luminescence of different polytypes strongly influenced by defects [1-3]. The luminescence spectra [4, 5] of SiC crystals and films with stacking faults (SF_i) in high-purity SiC [2] and with deep level (DL_i) [6-9] in lightly doped SiC reflect formation of intermediate metastable phases during 3C \leftrightarrow 6H transitions. SF_i and DL_i spectra hand-in-hand follow the structure transformations.

Grain boundaries in silicon carbide produced by sublimation were examined using high resolution

transmission electron microscope (HRTEM) [6]. 6H-SiC polytype boundary parallel to (0001) and 6H/15R hetero-polytype boundary with a thickness on the atomic level were observed. But luminescence of these defects was not investigated. Therefore, it is very important to investigate the grain boundaries (GB) by using optical methods.

Nowadays, since SiC thin films and crystals are widely used to fabricate devices, it is essential to understand properties of grain boundaries that can decrease the efficiency of these devices.

The purpose of this work is to decode the structure of low-temperature luminescence spectra in SiC crystals and in films with GB.

2. Experimental results and discussion

We studied low temperature spectra by using techniques described early [7]. For this experiment, we selected lumpy, blocky SiC crystals and crystals with steps of growth. The same type of spectra (GB) was observed, if crystals had block's disorientation in a basal plane (not only along the c axis). GB spectra are shown in Fig. 1 for the case when blocks have a common axis c , but were disoriented in the basal plane. Such GB spectrum is not observed in the thin plate-like crystals (not lumpy, not blocky crystals).

The low temperature photoluminescence spectrum of the SiC crystal which has blocks disoriented in the basal plane (concentration $N_D - N_A \sim 3 \cdot 10^{16} \text{ cm}^{-3}$, sample N2_{DL}) with GB spectrum at 4.2 ° K is shown in Fig. 1.

Thus, after detection of SF_i and DL_i spectra and their careful investigations [10-12], we found another new spectrum, which zero-phonon line had been allocated at 2.890...2.945 eV (the so-called GB spectrum) (Fig. 1). This spectrum, like to the cases of SF_i and DL_i spectra, clearly shows the fine structure. The GB spectrum was observed only in pure crystals, when the concentration of non-compensated impurities was $N_D - N_A \sim (2...9) \cdot 10^{16} \text{ cm}^{-3}$.

Fig. 2 shows the zero-phonon structure of the GB spectrum for different crystals of DL_i (Fig. 2a) and SF_i series (Fig. 2b). It can be seen that GB spectrum is very structured (see inset in Fig. 2a, where one segment equals 1 meV). The slit width (equal to 0.5 meV) yields to the detailed spectrum fractures and allowed to see the fine structure. In the particular case (sample N14_{DL}), the nature of GB spectrum is maximally manifested. The inset (Fig. 2a) shows an enlarged part of the zero-phonon GB spectrum (photoluminescence (PL) and phosphorescence (PS)) for the sample N2_{DL} with $N_D - N_A \sim 2 \cdot 10^{16} \text{ cm}^{-3}$ and for the sample N4_{DL} with $N_D - N_A \sim 8 \cdot 10^{16} \text{ cm}^{-3}$. We studied two polar faces of the crystals: (000 $\bar{1}$) and (0001). The chain curve 1 at the inset in Fig. 2a shows photoluminescence of the lumpy side of the crystal (there are a spiral, stage); the dashed curve 2 is PL of the mirror part of the crystal. Thus, graphs show GB spectra consisting of two bands.

In the very pure or perfect crystals (where there is only a spiral of growth, and there are no inconsistent borders), the GB spectrum does not exist. For example in the sample N1_{DL} [7], there was only a spiral of growth without grains, and there were no GB spectra. Also, we could not find the GB spectrum, if the acceptor impurity was less or of the order of 10^{16} cm^{-3} , and donor impurity was less than or of the order of 10^{16} cm^{-3} (*i.e.*, if there was not practical compensation, and samples really were very pure). The new GB spectrum was clearer pronounced in SF_i series just because compensation of the impurities in this series is virtually absent – there was a very low concentration of the acceptor impurity.

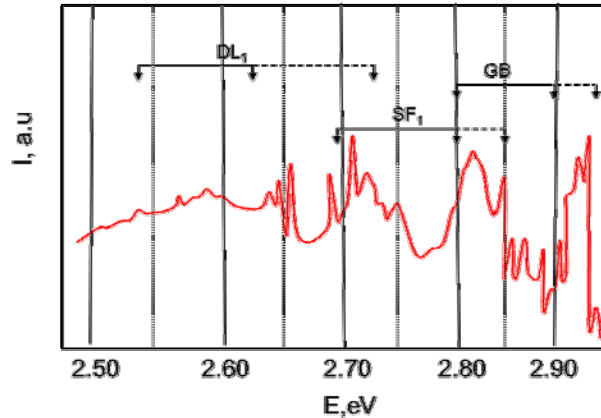


Fig. 1. GB type photoluminescence spectra of the sample N2_{DL} with $N_D - N_A \sim 3 \cdot 10^{16} \text{ cm}^{-3}$ at 4.2 K.

Plastic deformation was also carried out (Fig. 2c). Redistribution of the intensities in the structural part of the GB spectrum takes place like to that in the case of CdS. That is, when silicon carbide crystal was undergone to a large bend (twisted into a ram's horn), the island of the silicon carbide crystal (or its piece) became a kind of direct-gap band semiconductor (as it lifted the ban because of the phonons). It means that in this island phonon is not required, and there takes place the zero-phonon transition. (This is the same as in CdS.)

In crystals with the impurity concentration $N_D - N_A > 3 \cdot 10^{17} \text{ cm}^{-3}$, $N_D > 10^{18} \text{ cm}^{-3}$ (Fig. 3), GB spectra was not seen since refers to shallow levels of luminescence centers, like to SF_i spectrum. GB range can be observed simultaneously with those of SF_i and DL_i spectrum in impurity conditions (a) and (b) – Table (Fig. 3).

So, in case of GB spectra (similar to the case of DL_i and SF_i) the fine structure has allowed to define the boundaries of the zero-phonon part of the spectrum. GB have a line structure with the same density, stockade, which were observed in [11]. It indicates that the GB spectra represent incoherent boundaries. The GB spectra reflect locations of two matrices docking (the side mosaic's docking). Literally, it's non-compliance of the border (border inconsistencies in films). The rest part of the spectrum is described by involving phonon replicas at the edge of the Brillouin zone TA-46, LA-77, TO-95 and LO-104 meV, like to the other shallow centers (as in SF_i). But, unlike SF_i spectra, availability of non-phonon part here (in GB) in explicit manifestation indicates luminescence center locality rather than ply, extended character inherent to SF_i centers.

The temperature range of existence of the GB center (4.2...40 K) is similar to the shallow SF_i-centers.

The dependence of the GB spectra appearance (Fig. 3) on the degree of structural disorder δ -I, δ -II is sometimes observed and sometimes is not observed. Therefore, we can say that the dependence on the degree of structural disorder is not fixed.

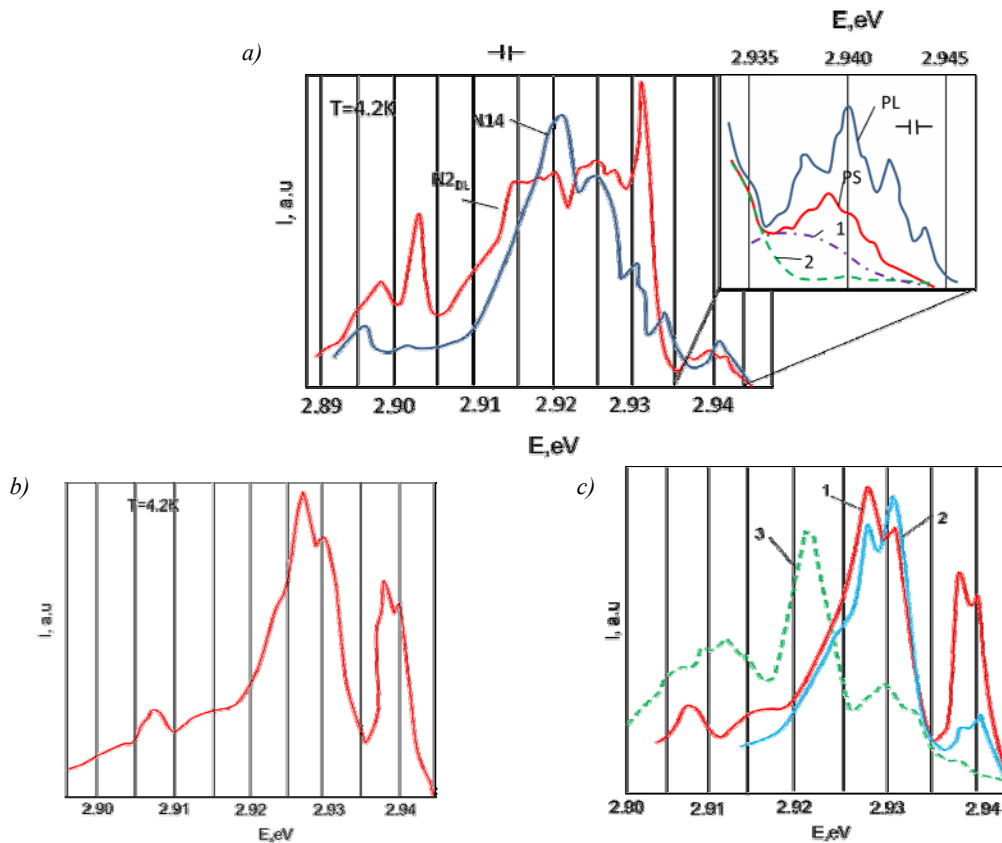


Fig. 2. The zero-phonon structure of the GB spectrum for different crystals: **a)** DL_i series for samples with $N_D - N_A \sim (2 \dots 8) \cdot 10^{16} \text{ cm}^{-3}$, $N_A \sim (2 \dots 7) \cdot 10^{17} \text{ cm}^{-3}$. The inset shows an enlarged part of the zero-phonon GB spectrum (photoluminescence (PL) and phosphorescence (PS), $\tau = 3 \text{ ms}$) for the sample $N2_{DL}$ with $N_D - N_A \sim 2 \cdot 10^{16} \text{ cm}^{-3}$ and for the sample $N4_{DL}$ with $N_D - N_A \sim 8 \cdot 10^{16} \text{ cm}^{-3}$ from two polar faces of the crystal $(000\bar{1})$ and (0001) . The line 1 describes photoluminescence of the other side of the crystal (lumpy), where there is a spiral, stage; 2 – PL of the mirror part of the crystal. **b)** SF_i series for most pure samples with $N_D - N_A \sim (4 \dots 9) \cdot 10^{16} \text{ cm}^{-3}$, $N_A < (1 \dots 3) \cdot 10^{16} \text{ cm}^{-3}$. **c)** GB spectrum (1) before plastic deformation (PD) and (2) after plastic deformation (PD) combined with (3) calculated the zero-phonon part of the SF_i spectrum [6].

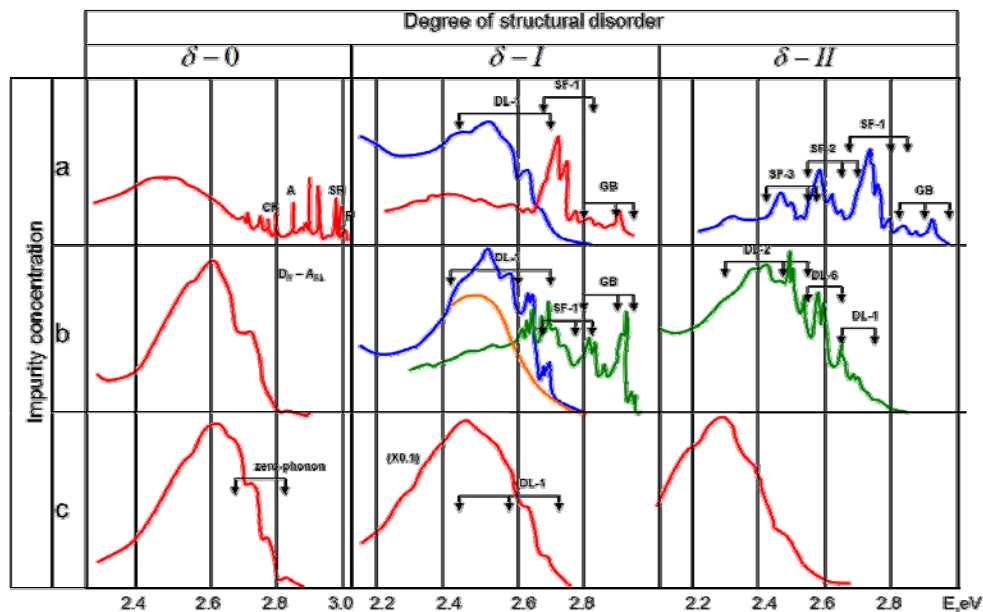


Fig. 3. Low-temperature photoluminescence spectra according to the structural imperfection and impurity concentration in SiC crystals and films. Zero-phonon parts: $SF_1 - 2.853 \dots 2.793 \text{ eV}$, $DL_1 - 2.730 \dots 2.625 \text{ eV}$, $GB - 2.945 \dots 2.890 \text{ eV}$. **a)** Pure SiC crystals and films with non-compensated concentration $N_D - N_A \sim (4 \dots 9) \cdot 10^{16} \text{ cm}^{-3}$, $N_A \sim (1 \dots 3) \cdot 10^{16} \text{ cm}^{-3}$; **b)** lightly doped samples with $N_D - N_A \sim (2 \dots 8) \cdot 10^{16} \text{ cm}^{-3}$, $N_D \sim (2 \dots 7) \cdot 10^{17} \text{ cm}^{-3}$; **c)** doped samples with $N_D - N_A > 3 \cdot 10^{17} \text{ cm}^{-3}$, $N_D > 10^{19} \text{ cm}^{-3}$.

The impurity concentration in the crystal affects the appearance and manifestation of the GB spectrum. If the impurity concentration is low in pure samples (Fig. 3a), the fine structure in the GB spectrum is generally observed, but it is weakly pronounced. With impurity concentration increase (Fig. 3b), the GB spectrum is more pronounced, and there is a clear expression of the fine structure in the spectrum. In the heavily doped crystals, the GB range is not observed (Fig. 3c).

Thus, GB spectra can be observed simultaneously with the SF_i and DL_i spectra in the case of pure and lightly doped crystals (a) and (b) in Fig. 3. In the heavily doped crystals (Fig. 3c), GB spectra are not observed.

The zero-phonon spectrum part of GB is located at the energy of 2.95...2.89 eV and has the most pronounced fine structure in the case of lightly doped crystals (Fig. 3b). The maximum resolution of the fine structure in the spectra of GB is defined as $\Delta H = 0.5$ meV (equal to half-width of the fine-structure elements).

The GB spectrum is shown through interaction with edge phonons TA-46, LA-77, TO-95, LO-104 meV within the temperature range (4.2...40 K). As the temperature increases, synchronous thermal decay of all elements of the fine structure is observed. The thermal activation energy of extinguishing is equal to $E_a^T = 7$ meV.

The dependence of the luminescence intensity on the excitation light intensity is expressed as $I_{lum} = I_{exc}^\alpha$, $\alpha = 0.7$. (Radiation of high-pressure mercury lamp was varied in the range of two orders of magnitude.) There is a differentiated change in the intensity of the fine structure. Namely, the short-wave part of the thin structure decreases quickly.

Luminescence intensity distribution (I_{lum}) on the elements of the fine structure is the same as at $\tau = 3$ ms in the attenuation at $I_{exc} = 0.004 I_0$. (The energy E_{exc} is higher than that or equal to 3.05 eV.)

Character of change in the damping (with different delay times τ) in the afterglow in the range of $\tau = 3...15$ ms is $I = I_0 \tau^{-\alpha}$.

Values of α are the same as in the case of DL_i, for the same range of τ [8]. Also, there is a differentiated variation of the fine structure intensity. Namely, the short-wave part falls faster.

Maximal total intensity of the GB spectrum decrease takes place, if excitation light polarization is parallel to the c axis of the crystal. Thus, the luminescence intensity decreases with polarization of the exciting light parallel to the c axis.

Plastic deformation of the crystal (three-point bending) stimulates the appearance of the GB spectrum or strengthening the existed GB spectrum. Plastic deformation of SF_i series, having initially GB range, amplifies them or stimulates their appearance. There is redistribution of the intensities in the fine structure in pure crystals (Fig. 3a). Namely, the intensity of the most short-wave part of the spectrum is noticeably reduced. In cubic β -SiC crystals, we observed occurrence of GB spectra after high temperature annealing.

3. Conclusion

By comparing the spectra SF_i, DL_i and GB in different conditions of registration and after various treatments of the crystal we can make the following conclusions.

1. Behavior of SF_i, DL_i and GB spectra is different. The zero-phonon part of GB spectrum does not follow restructuring of the crystal. The zero-phonon part of GB spectra does not fit in the dependence of its position in the energy scale on the percent of hexagonally as in the cases of SF_i and DL_i spectra. GB spectra are always in the same energy range (2.890...2.945 eV). It indicates that the GB spectra are characteristic for the grain boundaries. In the whole, mosaic interphase transformation of the GB spectra reflects the grain, interlayer boundaries in SiC crystals and films. The GB spectra are associated with luminescence centers localized in areas of specific structural abnormalities of the crystal, without no reference to the one-dimensional layer disordering (as SF_i and DL_i).

2. The GB spectra are the most intense and structurally expressed in crystals of DL_i series in samples with a lumpy growth terraces (staggered) from several centers. The GB spectra are observed in crystals with certain structural requirements and the impurity situation $N_D - N_A \sim (4...9) \cdot 10^{16} \text{ cm}^{-3}$, $N_A \sim (1...3) \cdot 10^{16} \text{ cm}^{-3}$; and especially in lightly doped samples with $N_D - N_A \sim (2...8) \cdot 10^{16} \text{ cm}^{-3}$, $N_D \sim (2...7) \cdot 10^{17} \text{ cm}^{-3}$. In the case of doped samples with $N_D - N_A > 3 \cdot 10^{17} \text{ cm}^{-3}$, $N_D > 10^{19} \text{ cm}^{-3}$, the GB spectra are not observed (Fermi level is raised). These spectra may occur simultaneously with the DL_i spectra and SF_i spectra. GB spectra also occur after high temperature processing of β -phase (in the 3C-SiC), with appearance of the α -phase, but much lower intensity with weak fine structure.

3. There observed is the zero-phonon part 2.945...2.890 eV with a fine structure. The edge phonons of the Brillouin zone TA-46 meV, LA-77 meV, TO-95 meV and LO-104 meV are involved in the development of the GB spectrum. The zero-phonon part 2.945...2.890 eV with a fine structure (in DL_i series of crystals) is better pronounced in crystals with the centers of origin growth of crystal with $N_D - N_A \sim (2...8) \cdot 10^{16} \text{ cm}^{-3}$, $N_D \sim (2...7) \cdot 10^{17} \text{ cm}^{-3}$.

4. The temperature range of observation is 4.2...40 K, *i.e.* about the same as in the case of part SF-II of calculated SF_i zero-phonon [6]. There is a synchronous thermal quenching of all elements of the fine structure. The thermal activation energy of quenching is $E_a^T \sim 7$ meV (it also coincides with the SF-II part of calculated zero-phonon of SF_i [6]).

5. Plastic deformation of the crystal (three-point bending) stimulates appearance of GB spectra. Plastic deformation of SF_i series crystals, having initially GB range, strengthens the GB spectra. There is redistribution of the intensities in the fine structure. The intensity of the most short-wave part of the spectrum is noticeably reduced.

References

1. Latu-Romain L., Ollivier M. *Silicon Carbide One Dimensional Nanostructures*. Wiley-ISTE, 2015.
2. Vlaskina S.I., Kruchinin S.P., Kuznetsova E.Ya., Rodionov V.E., Mishinova G.N., Svechnikov G.S. Nanostructure in silicon carbide crystals and films. *Int. J. Mod. Phys. B*. 2016. **30**. P. 1642019 (8 pages).
3. Choyke W.J., Matsunami H., Pensl G. *Silicon Carbide: Recent Major Advances*. Technology & Engineering, Springer, 2013.
4. Fei Yan, *Low Temperature Study on Defect Centers in Silicon Carbide*. Dissertation, University of Pittsburgh, 2009.
5. Zsolt Zolnai, *Irradiation-induced crystal defects in silicon carbide*. Ph.D. Thesis, Budapest University of Technology and Economics Department of Atomic Physics, MTA MFA – BUTE DAP, 2005.
6. Vlaskina S.I., Mishinova G.N., Vlaskin V.I., Rodionov V.E., Svechnikov G.S. 8H-, 10H-, 14H-SiC formation in 6H-3C silicon carbide phase transitions. *Semiconductor Physics, Quantum Electronics and Optoelectronics*. 2013. **16**, No. 3. P. 272–278.
7. Vlaskina S.I., Mishinova G.N., Vlaskin V.I., Rodionov V.E., Svechnikov G.S. Nanostructures in lightly doped silicon carbide crystals with polytypic defects. *Semiconductor Physics, Quantum Electronics and Optoelectronics*. 2014. **17**, No. 1. P. 155–159.
8. Vlaskina S.I., Mishinova G.N., Vlaskin V.I., Rodionov V.E., Svechnikov G.S. Structure of photoluminescence DL-spectra and phase transformation in lightly doped SiC crystals and films. *Semiconductor Physics, Quantum Electronics and Optoelectronics*. 2015. **18**, No. 2. P. 221–226.
9. Vlaskina S.I., Mishinova G.N., Vlaskin V.I., Rodionov V.E., Svechnikov G.S. External impacts on SiC nanostructures in pure and lightly doped silicon carbide crystal. *Semiconductor Physics, Quantum Electronics and Optoelectronics*. 2015. **18**, No. 4. P. 448–451.
10. Yoichi Ishida, Hideki Ichinose, Yoshizo Inomata. *Grain Boundaries in High-Purity Silicon Carbide*. eBook Silicon Carbide Ceramics-1. P. 169–183.
11. Cheng C., Heine Volker and Needs R.J. Atomic relaxation in silicon carbide polytypes. *J. Phys.: Condens. Matter*. 1990. **2**, No. 23. P. 5115.
12. Vlaskina S.I., Mishinova G.N., Vlaskin V.I., Svechnikov G.S., Rodionov V.E. Peculiarities of photoluminescence spectra behavior in SiC crystals and films during phase transformations polytypic defects. *Semiconductor Physics, Quantum Electronics and Optoelectronics*. 2016. **19**, No. 1. P. 62–66.